# Bilayer Rayleigh–Marangoni convection: transitions in flow structures at the interface

By Alex X. Zhao[1], Claus Wagner[2], Ranga Narayanan[1] and Rainer Friedrich[2]

[1]*Department of Chemical Engineering, University of Florida, Gainesville, FL 32611, USA*

[2]*Lehrstuhl für Strömungsmechanik, T.U. München, Arcisstrasse 21, D8000 München 40, Germany*



The fluid physics of buoyancy-driven (Rayleigh) and interfacial tension-driven (Marangoni) convection is examined for two superimposed layers of fluids. This convection occurs on account of temperature gradients that are imposed perpendicular to the fluid–fluid interface. Interfacial deflections, small as they may be, play an important part in identifying the mechanism that governs the flow, and calculations have been made that indicate whether hot or cold fluid flows towards or away from a crest or a trough. As a result, four possible flow structures or 'modes' at the interface have been identified. Two heating styles, heating from below and above, are considered and the behaviour of the fluid physics as a function of total fluid depths, depth ratios and gravity levels is explained. Changes in modes result because of changes in these parameters. We have given plausible physically based arguments that predict the sequential change in modes as these parameters are changed and have 'verified' our conjectures with calculations. Flow mechanisms in the case of a solidifying lower phase have also been studied, as this has an application to liquid-encapsulated crystal growth. Where convection is deemed detrimental to crystal homogeneity, we conclude that the liquid-encapsulated method of crystal growth is best conducted under Earth's gravity.

## 1. Introduction

This paper is concerned with the study of convection in fluid bilayers. Interfacial-driven convection must necessarily involve at least two fluid layers and we could well imagine that the fluid physics of motion, driven by interfacial tension and density gradients, depends largely on the heating direction, fluid depths as well as property ratios. One motivation for this study stems from an interest in liquid-encapsulated crystal growth where a vertical cylinder with thermally insulated side walls encloses the melt. The crystal solid phase can be below the melt phase and this corresponds to the bottom seeding situation where the liquid melt is now heated from above. An encapsulant is often placed above the melt in order to provide a diffusion barrier to high volatile constituents in the melt. An example is the growth of gallium arsenide, wherein arsenic is the highly volatile component and boron oxide the encapsulant. A bilayer with a common interface is thereby created. As a temperature gradient is applied across the interface, there are basically two mechanisms which can generate

*Proc. R. Soc. Lond.* A (1995) **451**, 487–502

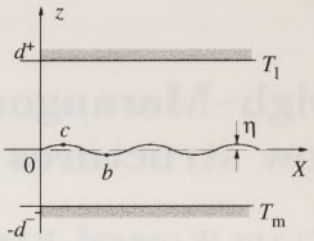


Figure 1. Schematic of the bilayer system. Dashed line is the flat interface in the quiescent state.



convection, i.e. buoyancy and interfacial tension gradients. These two mechanisms are called Rayleigh and Marangoni effects, respectively. In a model problem we could apply a temperature gradient that is either parallel or antiparallel to the gravitational field and the configuration represents an instability problem which is associated with a bifurcation from the quiescent state to the convective state. By applying a linear stability theory, we get the sufficient conditions for the onset of convection as well as the most dangerous wavelength of an imposed infinitesimal disturbance.

We can understand the physical mechanisms which are involved in interfacial tension gradient convection by considering a bilayer configuration, as shown in figure 1. Let $T_1 > T_m$ and further assume that gravitational effects are negligible. Now suppose we give a perturbation to an erstwhile flat interface so that the temperature at the point 'c' is higher than at 'b'. As most fluid bilayers have a negative interfacial tension gradient, the interfacial tension at 'c' will be lower than at 'b' and fluid is driven from 'c' to 'b'. Fluid from both phases must then rush towards 'c' and the final steady state will depend on the fluid property ratios and heights. If we have a liquid–gas system where the upper gas phase is assumed to be passive, then only liquid from below will move towards 'c' and it follows that unless the temperature gradient is reversed, the perturbations must decay. Gravity stabilizes or not according to the heating arrangement. It may be pointed out that the mechanism for flow can take place even if the interface is always restricted to be flat because temperature perturbations are still allowed. However, our interest will mainly focus on the general case where interfacial deformations are included.

## 2. Earlier work on bilayer convection

The first theoretical work in Marangoni convection was by Pearson (1958), wherein the liquid layer was assumed to be superimposed by a quiescent gas. One of the early studies in bilayers was by Sternling & Scriven (1959), who considered the pure Marangoni problem using mass transfer as an analogue to heat transfer, and Smith (1966), who examined the case of thermocapillary and gravity waves. Sternling & Scriven found that convection or instability can occur if the transfer takes place in either direction. This problem was later extended to include surface deflection and surface viscosity, but it was then assumed that the upper phase was passive.

This work was followed by Zeren & Reynolds (1972), who determined the critical temperature gradient for the onset of convection in a bilayer of water and benzene in order to compare theory with experiment. Now, in dimensionless form, the critical temperature gradient is represented by either the Marangoni or the Rayleigh number. As these groups are related to each other by a factor that contains physical properties, it is sufficient to calculate either the critical Rayleigh or critical Marangoni number

for the onset of convection. When the bilayer was 'heated from below', Zeren & Reynolds (1972) found that the onset of convection was either a buoyancy-driven flow generated from the upper phase or an interfacial tension gradient-driven flow that started at the interface. When they considered the case of a low liquid layer depth of the lower layer compared with the thickness of the upper layer, they found that the Marangoni convection in the bilayer served to delay the onset of motion and that the flow was primarily a buoyancy mechanism which was driven from the upper layer. This resulted in vertical stacking in the upper layer where the upper cell in the upper layer was associated with the buoyancy mechanism. On the other hand, when high depth ratios of the lower phase were considered, the onset of flow was due primarily to a Marangoni mechanism and not influenced much by the Rayleigh effect.

Following the work of Zeren & Reynolds (1972), Ferm & Wollkind (1982) performed detailed calculations for the silicone oil–air system with the hope of comparing their results with the experiments of Koschmieder (1967) and Palmer & Berg (1971). All calculations were performed for the case of the bilayer being 'heated from below'. In an effort to trace where the Marangoni regime was distinct from the Rayleigh regime, a series of calculations were performed and plotted as the critical temperature gradient against the depth of lower layer. They claimed that a drastic change in slope of this curve indicated the depth ratio of the lower layer when one mechanism took over the other.

Recent work on bilayer convection includes the interesting studies of Rasenat *et al.* (1989) and Wahal & Bose (1988). Rasenat *et al.* (1989) investigated the case of negligible surface deflections and uncovered oscillatory behaviour. They also considered a case of finite interfacial deflections but with negligible interfacial tension. While it may be argued that interfacial deflections are very small in comparison to the fluid depths, it is our view that the interfacial morphology helps to identify the controlling factors of competing convective mechanisms. This is what we aim to show in the subsequent sections.

It is noted that Zeren & Reynolds (1972) calculated the energy contributions from the buoyancy and surface mechanisms, as well as the critical Rayleigh and corresponding Marangoni numbers, in an effort to trace the leading characteristics of the flow. It is obvious that the energetics of the flow are calculated across the entire domain of the flow field and give some useful global information. However, it is also possible to consider the local behaviour of the flow at the interface using linear stability methods and by evaluating the eigenfunctions. We feel that this leads to vital information on the flow mechanism at the interface. In particular, we can, as we shall see, decide whether we have hot or cold fluid rushing towards or from a crest or a trough. We will observe that we can have four possible flow modes at the interface. This paper concerns operating parameters and, as we change the gravity level, the total depth or depth ratio, a sequential change of flow structures is obtained. The generality of this sequence depends on whether we have a liquid–gas system, a liquid–liquid system and whether the bilayer is 'heated from below or above'. The order of flow structures as we change these parameters also depends on whether the temperature coefficients of interfacial tension and density are negative or positive. From this we can decide whether the flow mode at the interface is promoted by Rayleigh or Marangoni effects.

## 3. Theoretical development

The model that we analyse is schematically shown in figure 1. The governing equations are derived in a manner identical to that of Ferm & Wollkind (1982) and so we dispense with the intermediate details in the cause of brevity. Without loss of generality, we introduce a two-dimensional coordinate system. In this system, the direction of the gravitational acceleration corresponds to the negative $z$-direction. The position of the deflecting interface is a function of $x$ and the time $t$ and is measured from the datum $z = 0$. The upper fluid is designated with + and the lower fluid with −, so that $d^+$ represents the vertical depth of the upper fluid and $d^-$ the depth of the lower fluid. The lower solid–liquid boundary has a constant temperature $T_\mathrm{m}$ and the upper solid surface has a temperature of $T_1$, respectively. The static interface has a temperature of $T_\mathrm{i}$. We will use the Boussinesq form of the continuity, Navier–Stokes and energy equations.

In order to get non-dimensionalized forms of the above equations, we introduce the scale factors for distance, velocity, time and pressure. These are $d^-$, $\kappa/d^-$, $(d^-)^2/\kappa$ and $\mu\kappa/(d^-)^2$, respectively. $\kappa$ and $\mu$ are the thermal diffusivity and dynamic viscosity of the lower phase, respectively.

The dimensionless temperature $\Theta$ is defined as

$$\Theta = \frac{(T - T_\mathrm{i})}{(T_\mathrm{m} - T_\mathrm{i})}. \tag{3.1}$$

In what follows, several important dimensionless groups will arise. These are the Rayleigh number $R$, Marangoni number $M$, Cripsation number $C$, the Bond number $G$ and Prandtl number $P$. They are defined as follows:

$$R = \frac{g\alpha\beta d^4}{\kappa\nu}, \quad M = \frac{\sigma_1\beta d^2}{\kappa\mu}, \quad C = \frac{\mu\kappa}{\sigma_0 d}, \quad G = \frac{\Delta\rho g d^2}{\sigma_0}, \quad P = \frac{\nu}{\kappa}.$$

All the physical properties in these numbers are referred to the lower phase. Here $\alpha$ is the negative thermal expansion coefficient, $\beta$ is the temperature gradient in the static state, $\nu$ is the kinematic viscosity, $\Delta\rho$ (i.e. $\rho^- - \rho^+$) is assumed to be positive, thereby excluding the Rayleigh Taylor instability. $g$ is the gravitational constant. $\sigma_0$ and $\sigma_1$ are the interfacial tension and its temperature coefficient, respectively.

The governing equations are nonlinear and admit the conductive quiescent state as a trivial solution. We linearize the equations about the trivial base state, eliminating all of the dependent variables in favour of the vertical component of velocity and temperature. Linearization of a dependent variable $\boldsymbol{A}$ gives

$$\boldsymbol{A} = \boldsymbol{A}_\mathrm{c} + \epsilon\boldsymbol{A}' + O(\epsilon^2), \tag{3.2}$$

where $\boldsymbol{A}_\mathrm{c}$ is the quiescent state and $\epsilon$ is a deviation from this state. $\boldsymbol{A}'$ is further decomposed as

$$\boldsymbol{A}' = \boldsymbol{A}_0(z)\mathrm{e}^{qt}\mathrm{e}^{\mathrm{i}\omega x}. \tag{3.3}$$

This means that a Fourier transform in the $x$-direction and a Laplace transform in time has been used. The dependent variables are the transformed temperature $\Theta_0$, the transformed vertical component of velocity $W_0$ and the transformed interfacial deflection $\eta_0$. We get the momentum and energy equations for the upper phase as

$$\frac{q}{P}(D^2 - \omega^2)W_0^+ = \frac{s}{r}(D^2 - \omega^2)^2 W_0^+ - aR\omega^2\Theta_0^+, \tag{3.4}$$

$$n(D^2-\omega^2)\Theta_0^+ = q\Theta_0^+ - \frac{W_0^+}{m}. \tag{3.5}$$

Here, $D$ represents the total derivative with respect to $z$. $r$, $s$, $a$, $n$ and $m$ are the density, kinematic viscosity, thermal expansion coefficient, thermal diffusivity and thermal conductivity ratios, respectively. These ratios are all referred to the lower phase properties as characteristic variables. The corresponding forms for the lower fluid are the same as the above equations with the '+' superscript replaced by the '−' superscript, and also with $r$, $s$, $a$, $n$ and $m$ replaced by unity. It is clear, by eliminating either dependent variable in favour of the other, that each phase is governed by a sixth-order ODE in either the temperature or vertical component of velocity. The boundary conditions are also transformed. For the sake of brevity we only give the interfacial conditions here. The kinematic, no slip and momentum equations at the interface are

$$W_0^+ = q\eta_0 = W_0^-, \tag{3.6}$$

$$[\![DW_0]\!]_-^+ = 0, \tag{3.7}$$

$$\left[\!\!\left[\frac{q}{P}K[r]DW_0 - K[s](D^2-\omega^2)DW_0 + 2K[s]\omega^2 DW_0\right]\!\!\right]_-^+ = (RC+G+\omega^2)\frac{\omega^2}{C}\eta_0, \tag{3.8}$$

$$[\![-K[s](D^2+\omega^2)W_0]\!]_-^+ = M\omega^2(\eta_0 - \Theta_0^-). \tag{3.9}$$

The continuity of temperature and heat flux at the interface are

$$[\![\Theta_0 - K[1/m]\eta_0]\!]_-^+ = 0, \tag{3.10}$$

$$[\![K[m]D\Theta_0]\!]_-^+ = 0. \tag{3.11}$$

$K[m]$ represents an operator that takes the value of $m$ in the upper phase and unity in the lower phase.

The above system represents an eigenvalue problem and has 10 dimensionless groups as parameters. It is sensible to concentrate on a particular system, fix the values of all the parameters and determine the critical condition of onset. As the Rayleigh number is related to the Marangoni number by a factor made up of physical properties, we can get the critical temperature gradient and critical wavelength of the disturbance for the chosen system.

The sign of the quantity $DW_0(0)/\eta_0$, called a flow indicator (cf. Smith 1966), tells us whether we have upflow or downflow at a crest. If it is positive, we have a downflow at a crest. The quantity $(\Theta-\Theta_c)_I/\eta$, which is of $O(\varepsilon^2)$ and equal to $\Theta_0/\eta_0$, is a temperature perturbation indicator and tells us that we have a hot spot at the crest if it is positive. Here $(\Theta-\Theta_c)_I$ is the dimensionless temperature perturbation at the interface. It is clear that there are four possible 'flow modes' or 'scenarios' and these words will be used interchangeably. These are depicted in figure 2 and assigned Roman numerals. The discussion of the numerical results will centre on these flow scenarios and the sequence of flow mode changes as we change the gravity level, the total depth $d_t$ and the depth ratio $\ell$ ($\equiv d^+/d^-$). The eigenfunctions $W_0^+(z)$ and $W_0^-(z)$ are also calculated and we can observe if there are any zeros in the $z$-direction. This will indicate if there is a vertical stacking of flow cells in either phase. The discussion of the physics assumes that $q = 0$ or the exchange of stability. By applying a spectral-$\tau$ method, it was shown that $\mathrm{Im}(q) = 0$ when $\mathrm{Re}(q) = 0$ in the cases studied.

The reliability of the numerical procedure was tested by recovering the results of

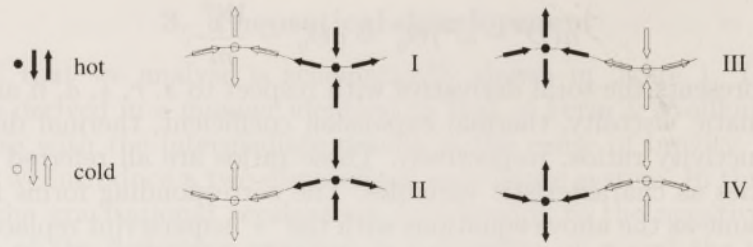


Figure 2. Four flow modes at the fluid–fluid interface. When the interface is flat, there is no difference between mode I and II, or mode III and IV.

Table 1. *Physical properties of fluids*

| parameter (units) | Dow Corning oil: under air | Dow Corning oil: above gallium | air above water or D.C. oil | water: under benzene (16 °C) | water: under air ($0^+$ °C) | benzene above water | gallium under D.C. oil |
|---|---|---|---|---|---|---|---|
| density ($g\ cm^3$) | 0.968 | 0.968 | 0.0012 | 0.998 | 0.999 | 0.884 | 6.09 |
| negative thermal expansion coefficient ($\times 10^{-4}\ °C$) | 9.6 | 9.6 | 34.0 | 2.06 | −0.68 | 14.5 | 1.0 |
| thermal conductivity ($\times 10^4$ erg $cm^{-1}\ s^{-1}\ °C^{-1}$) | 1.55 | 1.55 | 0.26 | 5.97 | 5.97 | 1.64 | 334.0 |
| thermal diffusivity ($\times 10^{-3}\ cm^2\ s^{-1}$) | 1.1 | 1.1 | 160 | 1.43 | 1.43 | 1.04 | 146.0 |
| kinematic viscosity (stoke) | 1.0 | 0.05 | 0.152 | 0.01 | 0.01 | 0.0067 | 0.003 54 |
| interfacial tension (dyne $cm^{-1}$) | 20.9 | — | — | 32.8 | 74.9 | — | 718.0 |
| negative interfacial tension gradient ($\times 10^{-2}$ dyne cm−1 °C) | 5.8 | — | — | 5.66 | 14.0 | — | 38.89 |

Zeren & Reynolds (1972) and Ferm & Wollkind (1982). Table 1 contains the fluid properties used in our calculations. The results for the silicone oil–air system agree with those of Ferm & Wollkind (1982) (within the round-off error). The comparison for the water–benzene bilayer shows good agreement with the values of Zeren & Reynolds (1972). We note that Renardy & Joseph (1985) and Wahal & Bose (1988) have independently verified these latter results.

## 4. Discussion of the numerical results

As we have used a linearized model, the calculations can only give information about the flow state at the onset of convection. The discussion is divided into several parts, each referring to the physical situation on hand. These are: (*a*) a liquid–gas case, as exemplified by the silicone oil–air system; (*b*) a liquid–liquid case, as depicted by the water–benzene system; (*c*) a case of two liquids in the presence of solidification, which is depicted by the gallium–silicone oil system with a solidifying gallium phase below; and (*d*) the situation that arises when the temperature coefficient of density is positive, as exemplified in the water–air system with the temperature range of water between 0 and 4 °C. As noted by Chandra & Holland (1983), there are some commercially important liquid semiconductors, such as mercury cadmium telluride, with positive temperature coefficients of density. It is clear from the choice of systems, where the upper layer is less dense than the lower layer, that the Rayleigh Taylor instability will be excluded from this study. Moreover, as neither phase is in motion in the base state, the Kelvin–Helmholtz instability is also excluded.

For a chosen system, the only control parameters in experiments are the total depths, depth ratio and gravity level. The critical temperature difference and critical wavelength at the onset are results that come from the linearized stability calculation. Before we discuss the results any further, we will clarify the roles of gravity, total depth and the parameter $\ell$. The lowering of gravity has the role of increasing the relative importance of Marangoni to Rayleigh effects and also reduces the Bond number or the effect of gravity waves. In this paper, different gravity levels will be chosen and a lowering of gravity will therefore reduce both gravity waves as well as the Rayleigh effect. Unlike Smith (1966), we will not study the case where only capillary and gravity waves are considered and where buoyancy is ignored. If the total depth is reduced for a given system, we have the effect once again of increasing the Marangoni effect relative to the Rayleigh effect in both phases. However, for a fixed total depth, decreasing $\ell$ has the role of increasing the Rayleigh effect in the lower phase at the expense of the Rayleigh effect in the upper phase. Besides, it also has the effect of increasing viscous resistance in the upper phase and this will play a role in the flow structure that the fluid bilayer system settles into. In what follows, we shall refer to figure 2, which shows four possible flow 'modes' or 'scenarios' at the interface at the onset of convection.

The actual 'mode' that a system settles into depends upon the thermophysical properties, gravity, total depth and depth ratio, but we will be less concerned about the mode that is realized and more concerned with the sequence of transitions from one mode to another as control parameters change and, therefore, will make general statements regarding this transition sequence for a variety of configurations. These statements will then be 'verified' by appealing to specific calculations on particular fluid–fluid systems and do not entail a mathematical proof.

It is instructive to note the relation between these modes. When the onset state of motion of the fluid bilayer goes from mode I to mode II, it simply means that a crest must gradually transform into a trough and the flow directions do not change at any particular lateral position along the interface. In going from mode II to mode III, two things happen: first, the crests and the troughs become progressively smaller and, second, the interface approaches the base state temperature. This change continues until the positions which were formerly crests now become troughs and vice versa. Meanwhile, the temperature perturbations also reverse in sign (cf. figure 2). Mode IV is seen only in one of the cases that we discuss, and changes to mode I under some

conditions. The transition between I and IV is similar to that between II and III. It is clear that the mode transitions must be smooth in the sense that the only way in which any two modes can coexist is in the asymptotic case where the interface is flat. Otherwise sudden mode transitions would imply the existence of codimension 2 points. It is easily seen that such codimension 2 points are precluded as the critical Marangoni number is simple, unique and obtained as the ratio of two determinants resulting from the imposition of the boundary conditions, while the corresponding eigenfunction is unique and this issue is made clear by Nadarajah & Narayanan (1987). In other words, we cannot ever get two or more coexisting flow modes at the critical Marangoni number for the laterally unbounded case.

There are some specific characteristics of the Marangoni and Rayleigh effects which are worth stating. First, if the Marangoni effect is operative alone then hot fluid at the interface must move towards the cold spot and the flow mode may be either I or II. Now, whether the hot region at the interface is a trough, as in mode I, or a crest, as in mode II, depends on the magnitude of the forces and the mechanical and viscous resistances in both phases. This is so as the interface at the hot spot will then bump towards the region that exerts the greater resistance to flow in that region. Second, if the Rayleigh effect is operative alone then matters become a little complicated. In the case of a liquid–liquid bilayer, the upper fluid offers resistance on account of its viscosity and density and yet it conducts heat. We can expect to see any of the modes depending on the forces at play and the magnitude of the resistance. As we continue to consider the pure Rayleigh effect, but now restrict the study to the 'heated from above' problem, it initially appears that no steady flow will occur unless we have the odd case of a positive thermal expansion coefficient. However, this premise can be shown to be false. We refer the reader to Gershuni & Zhukovitskii (1980). These authors discuss a case where the upper fluid is less conductive than the lower fluid and has also a much smaller thermal expansivity. In that peculiar case, we can see that a mechanical perturbation to the upper fluid sends a hot fluid element towards the interface, where it easily transmits heat to the more conductive lower region. This in turn excites buoyancy-driven motion in the lower phase and, as a result, momentum from the lower phase is transmitted to the viscous upper layer and the process continues. Because Gershuni & Zhukovitskii (1980) studied the case of water and mercury, we verified their results as a test of our numerical method, but otherwise did not consider this particular system further. In the unusual case where the lower fluid has a positive thermal expansion coefficient, we obtain mode IV for a liquid–gas system because it is easier to push light cold fluid upwards and towards the interface. We will now discuss these problems in the following sections and provide numerical evidence for various system calculations. In what follows, both buoyancy and interfacial tension gradients, in general, come into play unless noted otherwise.

### (*a*) *Liquid–gas system*

It is clear in the liquid–gas case that only modes I and II are possible candidates, as the upper fluid is virtually passive, offers little fluid mechanical resistance and hot fluid from below must flow upwards for the reason that this is the situation favoured by both buoyancy and interfacial tension gradient forces. Calculations that treat the upper gas as passive were compared with those that treat it as active and we obtained results that were within 1% of each other insofar as the values of the critical temperature difference were concerned.

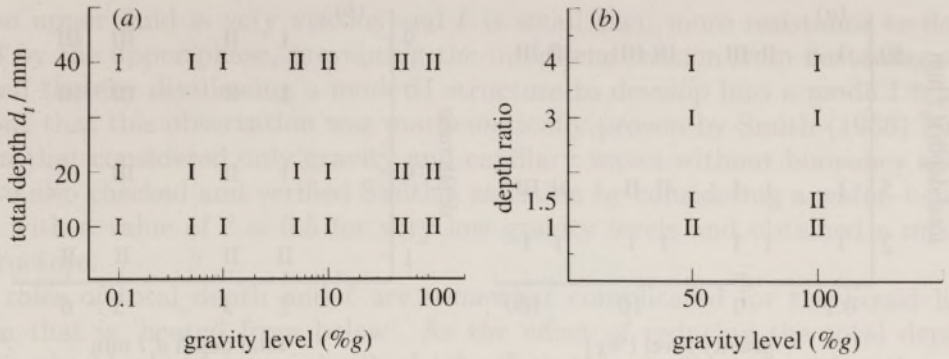


Figure 3. Mode switching for the liquid–gas (silicone oil–air) system 'heated from below': (*a*) the effect of gravity level and total depth ($\ell = 1$); (*b*) the effect of depth ratio ($d_t = 10$ mm).

If this system were 'heated from above' at the upper plate, then it would be very stable as calculations tell us that the critical negative temperature gradient is extremely large. This is contradictory to the experimental results of Block (1956) and we believe that the flow he had must have resulted from non-uniform heating or meniscus effects. For the case of 'heated from below', if the Marangoni mechanism alone is operative with negligible gravitational effects, then the flow will align itself into mode I as the resistance to flow is greater in the lower phase leading to a trough at the hot spot. If buoyancy alone were operative then either mode is possible depending on the mechanical and viscous resistance to flow offered by the lower phase. For example, if $\ell$ were large then mode I would be preferred, compared to mode II, since the hot spot would once again become a trough according to the criterion established earlier. On the other hand, if $\ell$ were small and the resistance decreased relative to the buoyancy then the system would align itself to mode II, giving rise to a situation where hot plumes rise towards a crest in order to balance the cold heavy fluid flowing down from a trough.

The modal transitions (in the combined Rayleigh–Marangoni case) must therefore proceed from II to I in figure 2 as we reduce gravity and, depending on the system, the reduction in gravity level may have to be significant. Figure 3*a* shows the flow modes as a function of gravity and depth levels for the silicone oil–air system and we observe that our arguments are validated by the numerical calculations. A calculation of the critical temperature gradients show a monotonic behaviour in the vicinity of the flow switch. In this regard, we agree with the conclusions obtained by Sarma (1987), who considered the upper phase to be truly passive.

From our earlier comments, we can see that a reduction in the total depth causes a relative increase of Marangoni to Rayleigh effects. We therefore see a transition from mode II to mode I as the total depth is decreased. For a fixed total depth and gravity level, an increase in $\ell$ should cause a decrease in the lower phase Rayleigh effect in comparison to the Rayleigh effect in the upper phase. But the upper phase is a gas and is largely passive and therefore an increase in $\ell$ can only cause a decrease in the overall Rayleigh effect, and by default it will encourage the Marangoni effect, thereby going from modes II to I, as seen in figure 3*b*.

A comment on Ferm & Wollkind's (1982) paper is in order. They performed a calculation in the silicone oil–air system to find the depth for the transition from Marangoni to Rayleigh dominant regimes. Using a value of $\ell = 0.109$ they obtained a value of $d^- = 6.5$ mm, whereas we obtain a value of 2.5 mm. It is to be noted that our notion of mechanism change is given by the flow scenarios as manifested

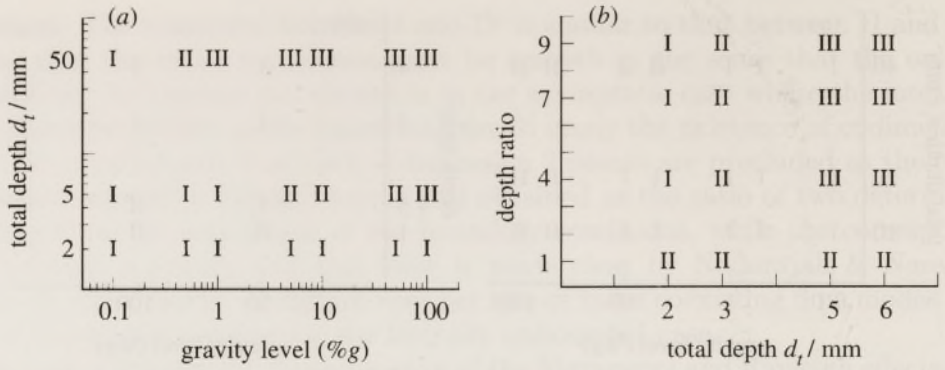


Figure 4. Mode switching for the liquid–liquid (water–benzene) system 'heated from below': (*a*) the effect of gravity level and total depth ($\ell = 4$); (*b*) the effect of depth ratio ($1g$).

in figure 2, and in the liquid–gas system we can only obtain the first two modes. Ferm & Wollkind (1982) indicated that the mechanism changed from Marangoni- to Rayleigh-dominant when there was a change in the slope of the graph between critical temperature gradient and lower phase depth. We feel that our classification is more definitive as it identifies various scenarios at the interface between both fluids.

### (*b*) *Liquid–liquid systems*

Liquid–liquid systems are interesting as they may be examined with two different heating directions and we choose the water-benzene system to explain the physics because it provides a good test case to verify the detailed results of Zeren & Reynolds (1982).

The modal sequence as we increase gravity, and also 'heat from below', goes from mode I to mode II and then to mode III. The reason why we can expect to see mode III as gravity is increased from mode II is because the Marangoni effect becomes less important and less work is required to push up the short cold columns seen in III as opposed to the tall cold columns seen in IV. In fact, mode IV occurs for the peculiar situation where the thermal expansion coefficient is positive, and this we will discuss later. The particular system that we have investigated has a large value of $a$, the thermal expansion coefficient ratio†, and therefore it is generally biased towards greater buoyancy in the upper phase in comparison to the lower phase, unless of course $\ell$ becomes so small so as to discourage buoyancy in the upper phase in favour of the lower phase. It is for this reason that, as gravity is increased from mode II, the fluid goes into mode III for all of the $\ell$ values that we have used. Further, it is at the point of mode switching that the Marangoni effect ceases to be of importance and this is seen by the fact that the fluid at the interface does not move from hot regions to cold regions. However, once the fluid is in mode III, the Marangoni effect delays the instability by raising the critical temperature difference. When the mode changes from mode II, upon decreasing gravity, then mode I, which is favoured by the Marangoni effect, is realized. It should be noted that the mode can remain in mode II and never change into mode I on the reduction of the gravity level. This peculiarity once again has to do with the value of $\ell$ and upon the viscosity ratio

† All of our calculations and statements in the case of liquid–liquid systems are restricted to the situation where the ratio of the upper phase thermal expansion coefficient to the lower one is much greater then unity. The reverse case is not discussed in the cause of brevity but the physically based arguments follow in a similar manner.

$s$. If the upper fluid is very viscous and $\ell$ is small then more resistance to flow is exerted by the upper phase, preventing the interfacial tension from flattening out a crest and thereby disallowing a mode II structure to develop into a mode I type. It turns out that this observation was mathematically proven by Smith (1966) for the problem that considered only gravity and capillary waves without buoyancy effects. We have also checked and verified Smith's assertion by considering a water–benzene bilayer with a value of $\ell = 0.5$ for very low gravity levels and obtained a mode II flow structure.

The roles of total depth and $\ell$ are somewhat complicated for the liquid–liquid problem that is 'heated from below'. As the effect of reducing the total depth is to favour the Marangoni over the Rayleigh effect, this simply means that the mode switching for this heating direction goes from mode III to mode II and then to mode I as total depth is reduced. Figure 4*a* bears this out. Of course, for very low $\ell$, mode II is obtained on account of the viscous-mechanical resistance to flow in the upper phase and figure 4*b* bears this out.

Now, if total depth and gravity are kept constant and $\ell$ alone is increased, physical reasoning demands that the buoyancy effect in the upper layer increases relative to the lower layer. Let us suppose that the fluid properties and conditions are such that the fluid settles into mode II. If the total depth is small† and we continue to increase $\ell$, we expect the flow to switch from mode II to mode I, because the interface gets closer to the hot lower surface in what is already a thin layer and the Marangoni effect plays a dominant role when the interface gets close to the lower hot surface, thereby giving rise to a hot trough. Meanwhile, in this thin layer, the large value of $\ell$ causes the Rayleigh effect in the upper layer to become more significant than in the lower layer. Buoyancy in the upper layer tends to cause hot plumes to rise in that layer, in opposition to the Marangoni-influenced flow at the interface. As a result, we see a vertical stacking of flow cells in the upper phase as $\ell$ is increased. The upper cell in the upper phase is a result of the buoyancy in that phase and the lower cell in the upper phase is a result of the Marangoni motion that results on account of the proximity of the interface to the lower heated surface. The cell stacking persists even as the mode switches from II to I. The effect of $\ell$ for a small total depth is seen in the left region of figure 4*b*, while figure 5 depicts the velocity and temperature eigenfunctions when vertical stacking takes place.

Contrast the situation discussed above with the case where the total depth is large; we then expect the fluid to switch from mode II to mode III as $\ell$ is increased and the explanation for this is as follows. The large total depth increases buoyancy in both phases; the upper phase being even more buoyant than the lower on account of two reasons. First, the increasing value of $\ell$ continues to enhance the buoyancy in the upper phase in relation to the lower and second, but less important, the value of $a$ is much greater than unity (in the systems that we chose to compute). As the upper layer is now very buoyant, it would require less work for the fluid to go into mode III, where a shorter column of fluid is pushed up against gravity in both phases, in contrast to the situation of mode II. Remember that a shorter column of liquid is pushed up against gravity in mode I as well, but the system would prefer mode III as the upper phase portrays more buoyancy in this mode as

† The notion of large total depth or small total depth is entirely system dependent and only calculations or experiments can determine how large the total depth should be for us to see what we predict. However, we can still make statements of a qualitative manner and verify them by calculations.

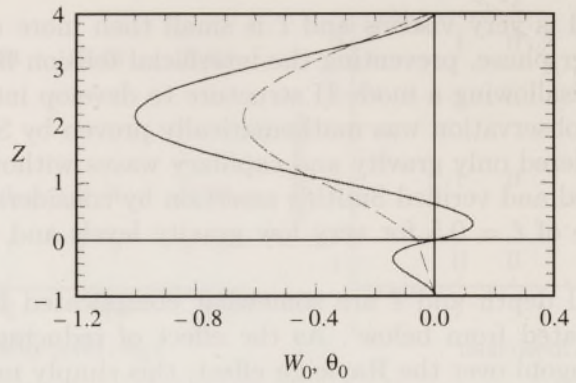


Figure 5. The perturbed axial component of velocity and temperature as a function of $z$-coordinate in a water–benzene system 'heated from below' ($1g$, $d_t = 2$ mm, $\ell = 4$): ——, velocity; – – –, temperature.

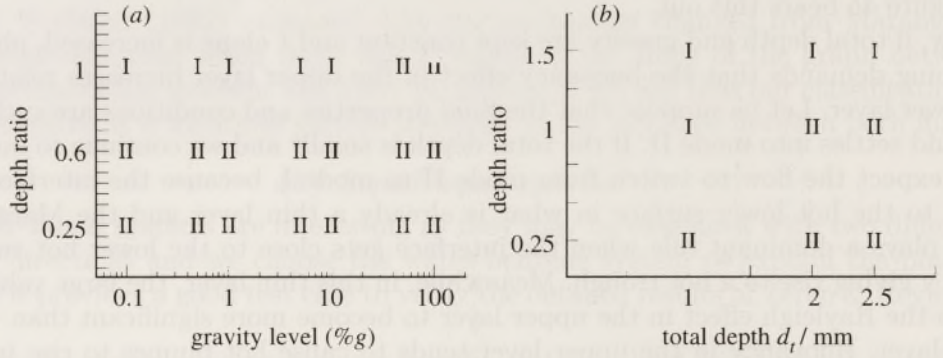


Figure 6. Mode switching for the liquid–liquid (water–benzene) system 'heated from above': (*a*) the effect of gravity level and total depth ($d_t = 2$ mm); (*b*) the effect of depth ratio ($1g$).

compared to mode I. The numerical calculations confirm the physical arguments, as seen in the right-hand region of figure 4*b*. In these cases, where a large total depth is considered, an increasing value of $\ell$ does cause the interface to get closer to the hot lower rigid surface, however it is not close enough to encourage an overriding effect of Marangoni-influenced motion, and that is why the system settles into mode III with cold troughs. At the intermediate values of total depth, mode II remains as expected for all values of $\ell$.

When the water–benzene bilayer is 'heated from above', we predict a sequence from mode I to mode II as we increase gravity; the explanation for this mode switch is as follows. 'Heating from above' causes convection that is started by a Marangoni influence and therefore the flow must necessarily be in either mode I or mode II. Meanwhile, gravity serves the purpose of stabilization and therefore delays the instability. Now the value of $a$, the thermal expansion coefficient ratio, is much greater than unity in the system studied and an increase in gravity causes an increase in the resistance to flow in the upper phase because of the stabilization effect. This in turn causes the switch into mode II, creating hot crests at the interface.

Likewise, for the 'heated from above' case, the mode switching goes from mode II to mode I as we decrease total depth for the reason that a decrease in total depth is tantamount to a decrease in the stabilizing Rayleigh effect in each phase, thereby enhancing the Marangoni effect. If we again consider gravity and total depth to remain constant but vary $\ell$ for the 'heated from above' case, we will go from mode II

to mode I as $\ell$ is increased. This mode switch will take place when the total depth is small, because an increase in $\ell$ has the effect of increasing the viscous resistance in the lower phase, even though it makes the upper phase more stabilizing than the bottom phase. When the total depth is large, the effect is mainly to make the upper phase stabilizing, thereby increasing the resistance there and so mode II remains intact for all $\ell$. Note, as a result of our reasoning, the 'heated from above' configuration cannot cause vertical stacking. Vertical stacking can occur only when both Marangoni and Rayleigh effects destabilize in a particular phase and yet when both act in opposition to each other in a 'flow direction' sense. This does not occur in the 'heated from above' configuration with a negative thermal expansion coefficient. Our thinking in the above is underscored by the numerical calculations that are presented in figures 6*a*, *b*.

A comment on Smith's (1966) paper is in order. His study was concerned with Marangoni convection in the presence of gravity waves but without a buoyancy mechanism. No mention was made of hot or cold spots and only modes where fluid from the lower phase moved upwards or downwards from a crest were considered. Yet a pair of sufficient conditions were obtained to indicate whether flow moved upwards or downwards into a crest. This was obtained by use of a flow indicator as in this study. All of our observations validated Smith's (1966) derived result.

### (*c*) *Solidifying phase below a liquid–liquid bilayer*

The third case is a modification of the 'liquid–liquid' problem that is 'heated from above'. It involves a solidifying phase below the lower layer of liquid. The condition at the boundary of the lower liquid and the adjacent solidifying phase is replaced by

$$D\theta_0^- = \omega\theta_0^- \coth(\omega\Lambda). \tag{4.1}$$

It is implicitly assumed that the rate of solidification is slow enough to be negligible and so that there is no net flow in the base state. The perturbed deflection of the solid–liquid interface is given by

$$\zeta_0 = \theta_0^- \tag{4.2}$$

In the above, $\Lambda$ is the dimensionless thickness of the lower solidifying phase, scaled with respect to the lower liquid thickness. We note that our calculations exclude the important situation where constitutional supercooling, as considered by Mullins & Sekerka (1964), is involved. The main result from our calculation is that the solid thickness of the lower phase does not affect the flow structure at $1g$ but does affect the flow at low gravity levels. In other words, the coupling is only one way at high gravity. We surmise that even though the solid thickness destabilizes the flow, it is insignificant compared to the overwhelming stabilization of gravity. This result is depicted in figure 7. It is apparent from this figure that solidification at lower levels of gravity may not prove beneficial at all under this heating arrangement as the critical temperature gradient is lowered in the low gravity state and convection is thereby enhanced. As a result, it appears that liquid-encapsulated crystal growth is better conducted under Earth's gravity conditions as the configuration would be more stable.

We can also determine whether the solid–liquid interface deflection is in phase or out of phase with the upper interface by examining the ratio $\zeta_{(0)}/\eta_{(0)}$. What is even more interesting is that when mode switching takes place as we increase gravity, we find that the deflection at the solid–liquid interface lower phase does not change sign.

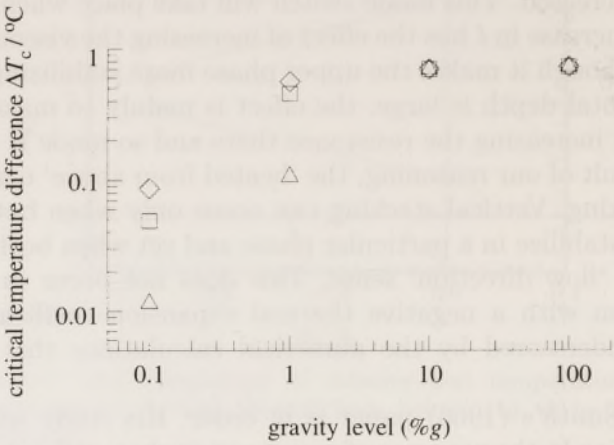


Figure 7. The effect of the solid thickness (i.e. $\Lambda$) on the onset temperature of a gallium–silicone oil system ($d_t = 5$ mm, $\ell = 0.25$) 'heated from above' for different gravity levels: △, $\Gamma = 10$; □, $\Gamma = 1$; ◇, $\Gamma = 0.01$.

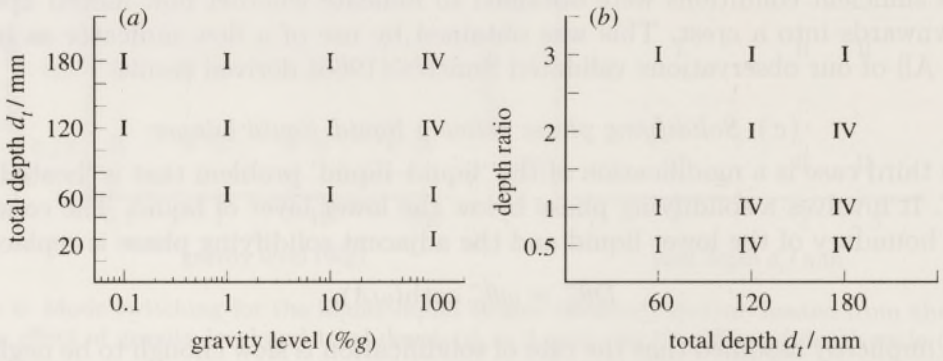


Figure 8. Mode switching for the liquid–gas (water–air) system 'heated from above'. The liquid in this system has a positive thermal expansion coefficient (water is between 0 and 4 °C): (*a*) the effect of gravity level and total depth ($\ell = 1$); (*b*) the effect of depth ratio ($1g$).

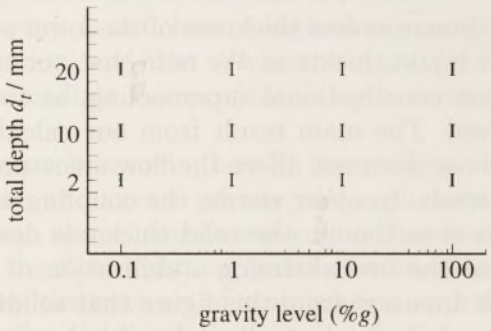


Figure 9. The effect of gravity level and total depth on mode switching for the liquid–gas (water–air) system 'heated from below' ($\ell = 1$). The liquid in this system has a positive thermal expansion coefficient (water is between 0 and 4 °C).

### (*d*) *The case of a system with a positive thermal expansion coefficient*

Finally, we consider the case of a system where the thermal expansion coefficient of the lower phase is positive. This is exemplified by the results using the water–air system, as shown in figures 8*a*, *b*. Here the heating can take place from above or below. If the heating is from above, the origin of the convection can only be due

Table 2. *Summary of mode switching*

| | negative thermal expansion coefficient in liquid | | | |
|---|---|---|---|---|
| | liquid–gas system 'heated from below' | liquid–liquid system 'heated from below' | | liquid–liquid system 'heated from above' |
| increasing gravity level | I → II | I → II → III | | I → II |
| increasing total depth | I → II | I → II → III | | I → II |
| increasing depth ratio $\ell$ | II → I | small total depth II → I | large total depth II → III | II → I |

| | positive thermal expansion coefficient in liquid | |
|---|---|---|
| | liquid–gas system 'heated from above' | liquid–gas system 'heated from below' |
| increasing gravity level | I → IV | I |
| increasing total depth | I → IV | I |
| increasing depth ratio $\ell$ | IV → I | I |



buoyancy as the upper layer is virtually passive. The flow, as expected, stays in mode IV for large gravity levels. While the convection is necessarily of buoyancy in origin, it is also true that the Marangoni effect plays a part in countering the flow, thereby delaying the instability. Since the strength of this interfacial mode of convection is dependent on the magnitude of the interfacial tension gradient, we can observe that at low gravity the Marangoni effect is dominant and, as gravity or total depths are reduced, the mode switches to I. Here Marangoni convection causes fluid to move from hot to cold regions at the interface and a shorter column of hot heavier water is balanced by a taller column of cold lighter water. As gravity decreases, the system becomes more stable (despite the change in the flow mode from IV to I) as evidenced by an increase in the critical temperature gradient, just as we would expect. If the water–air system were 'heated from below' so as to allow the temperature range across the water to be between 4 and 0 °C, then it is likewise argued that we would get mode I at all gravity levels, as shown in figure 9. Here the buoyancy stabilizes and the onset flow comes from the interfacial tension gradient. Much like the 'heated from below' configuration in the liquid–gas case for negative

thermal expansion coefficient and pure Marangoni flow, mode I will be the structure chosen by the system.

Table 2 gives a summary of the mode switching explained in the study. Once again, our results depend upon the thermophysical properties of the individual systems chosen in this study. However, the physically based arguments can be similarly made for other systems. We believe that it is valuable to make such arguments in order to identify the mechanisms that dominate the flow structure at an interface.

This work started from discussion during a visit sponsored by the A. v. Humboldt Foundation. C. Wagner was supported by NASA (Langley) grant NAG 1-1474. The work was completed under an NSF grant CTS 9307819. Computations were performed at the Pittsburgh Supercomputing Center.

## References

Block, M. J. 1956 Surface tension as the cause of Bénard cells and surface deformation in a liquid film. *Nature* **176**, 650–651.

Chandra, D. & Holland, L. R. 1983 Density of $Hg_{1-x}Cd_xTe$. *J. Vac. Sci. Technol.* A **1**, 1620–1624.

Ferm, E. N. & Wollkind, D. J. 1982 Onset of Rayleigh–Bénard–Marangoni instability: comparison between theory and experiment. *J. Non-equilibr. Therm.* **7**, 169–189.

Gershuni, G. Z. & Zhukhovitskii, E. M. 1980 Instability of a system of horizontal layers of immiscible fluids heated from above. Translated from *Izv. Akad. Nauk SSSR: Mekh. Zh.* i **6**, 28–34.

Gousebet, G., Maquet, J., Roze, C. & Darrigo, R. 1990 Surface tension and coupled buoyancy driven instability in a horizontal fluid layer—overstability and exchange of stability. *Physics Fluids* A **2**, 903–911.

Joseph, D. D. 1976 *Stability of fluid motions.* vol. I. New York: Springer.

Koschmieder, E. L. 1967 On convection under an air surface. *J. Fluid Mech.* **30**, 9–15.

Mullins, W. W. & Sekerka, R. F. 1964 Stability of a planar interface during solidification of a dilute binary alloy. *J. appl. Phys.* **35**, 444–451.

Nadarajah, A. & Narayanan, R. 1987 On the completeness of the Rayleigh–Marangoni and Graetz eigenspaces and the simplicity of the eigenvalues. *Q. appl. Math.* **XLV**, 81–92.

Palmer, H. J. & Berg, J. C. 1971 Convective instability in liquid pools heated from below. *J. Fluid Mech.* **47**, 779–787.

Pearson, J. R. A. 1958 On convection cells induced by surface tension. *J. Fluid Mech.* **4**, 489–500.

Rasenat, S., Busse, F. H. & Rehberg I. 1989 A theoretical and experimental study of double-layer convection. *J. Fluid Mech.* **199**, 519–540.

Renardy, Y. & Joseph, D. D. 1985 Oscillatory instability in a Bénard problem of two fluids. *Physics Fluids* **28**, 788–793.

Sarma, G. S. R. 1987 Interaction of surface tension and buoyancy mechanisms in horizontal liquid layers. *J. Thermophys. Heat Transfer* **1**, 129–135.

Scriven, L. E. & Sternling, C. V. 1964 On cellular convection driven by surface-tension gradients: effects of mean surface tension and surface viscosity. *J. Fluid Mech.* **19** 321–340.

Smith, K. A. 1966 On convective instability induced by surface tension gradients. *J. Fluid Mech.* **24**, 401–414.

Sternling, C. V. & Scriven, L. E. 1959 Interfacial turbulence: hydrodynamic instability and the Marangoni effect. *A.I.Ch.E. Jl* **5**, 514–516.

Wahal, S. & Bose, A. 1988 Rayleigh–Bénard and interfacial instabilities in two immiscible liquid layers. *Physics Fluids* **31**, 3502–3510.

Zeren, R. W. & Reynolds, W. C. 1972 Thermal Instabilities in two fluid horizontal layers. *J. Fluid Mech.* **53**, 305–327.

*Received 28 April 1994; revised 21 February 1995; accepted 28 February 1995*